



Observations and modelling of algal growth on a snowpack in northwest Greenland

Yukihiko Onuma¹, Nozomu Takeuchi², Sota Tanaka², Naoko Nagatsuka³, Masashi Niwano⁴, Teruo Aoki^{5,4}

5 ¹ Institute of Industrial Science, University of Tokyo, Chiba, 277-8574, Japan

² Graduate School of Science, Chiba University, Chiba, 263-8522, Japan

³ National Institute of Polar Research, Tokyo, 190-8518, Japan

⁴ Meteorological Research Institute, Tsukuba, 305-0052, Japan

⁵ Graduate School of Natural Science and Technology, Okayama University, Okayama, 700-8530, Japan

10 *Correspondence to:* Yukihiko Onuma (onuma@iis.u-tokyo.ac.jp)

Abstract. Snow algal bloom is a common phenomenon on melting snowpacks in polar and alpine regions and can substantially increase melting rates of the snow due to the effect of albedo reduction on the snow surface. In order to reproduce algal growth on the snow surface using a numerical model, temporal changes in snow algal abundance were investigated on the Qaanaaq Glacier in northwest Greenland from June to August 2014. Snow algae first appeared at the study sites in late June, which was approximately 94 hours after air temperatures exceeded the melting point. Algal abundance increased exponentially after the appearance, but the increasing rate became slow after late July, and finally reached 3.5×10^7 cells m^{-2} in early August. We applied a logistic model to the algal growth curve and found that the algae could be reproduced with an initial cell concentration of 6.9×10^2 cells m^{-2} , a growth rate of $0.42 d^{-1}$, and a carrying capacity of 3.5×10^7 cells m^{-2} on this glacier. This model has the potential to simulate algal blooms from meteorological data sets and to evaluate their impact on the melting of seasonal snowpacks and glaciers.

1 Introduction

Snow algae are cold-tolerant, photosynthetic microbes growing on snow and ice and are commonly found on glaciers and snowfields worldwide. Snow algal bloom occur on thawing snow surfaces and changes the colour of the snow to red or green (Thomas and Duval, 1995; Hoham and Duval, 2001; Takeuchi, 2013). Red snow algal bloom (usually by *Chlamydomonas* (*Cd.*) *nivalis*) commonly occur in polar and alpine snow fields (Hoham and Duval, 2001; Segawa et al., 2005; Takeuchi et al., 2006; Lutz et al., 2016; Tanaka et al., 2016; Ganey et al., 2017).

The conditions required for the growth of snow algae are the occurrence of liquid-water, solar radiation, and nutrients. Snow algal cells are typically present in the liquid water film surrounding snow grains when the snow melts (Fukushima, 1963). Field observations showed that snow algae begin to grow when the air temperature is above the freezing point for several days, suggesting that algal growth requires a certain amount of water content in the snow (Pollock, 1972; Onuma et al., 2016). A field study on algal photosynthesis suggested that algal growth requires at least 1% of incident photosynthetically active



radiation in the snowpack, promoting photosynthesis and germination of algae (Curl et al., 1972). After the algae appears on the snow surface, nutrient depletion (particularly nitrates) in the snowpack can cause shifts in life cycle phases and decrease the growth rate (Hoham et al., 1989). Previous studies have shown that the abundance of snow algae increases as the snow melts. For example, snow algal abundance on a glacier in Alaska continued to increase during the melting season until the snowpack completely melted on the glacier surface (Takeuchi, 2013). Snow algal abundance on a seasonal snowpack in Japan increased exponentially with snow melting until the snowpack completely melted (Onuma et al., 2016). Such temporal changes in snow algal abundance can be affected by the snow conditions, such as water content, solar radiation, and nutrient availability.

A numerical model could be utilized to reproduce the seasonal change in algal abundance on snowpacks, to understand algal growth in snowfields on a regional or worldwide scale, and to evaluate their effects on the surface albedo and resultant melting rate. The effect of algae on surface albedo can be physically calculated using an albedo model based on algal abundance (Cook et al., 2017a; 2017b). A temporal change in snow algal abundance could also be reproduced using a numerical model. Many models have been proposed and applied to temporal changes in the abundance of photosynthetic microbes in aquatic environments such as lakes or oceans. For example, there has been a model for cyanobacteria in lakes, which can reproduce their exponential growth using their initial concentration, growth rate, and nutrient concentration (Chen et al., 2009). Additionally, a model for algae (diatoms) growth in sea ice was developed using a sea ice physical model (Pogson et al., 2011). This model can reproduce the temporal change in chlorophyll a concentration in Arctic sea ice from the initial chlorophyll a concentration, algal growth rate, and grazing rate. The exponential growth of snow algae observed on a seasonal snowpack in Japan was reproduced using a Malthusian model (Onuma et al., 2016). Although this model might be effective for the seasonal snowpacks that exist for a short period and disappear in spring or early summer, it is questionable whether the model is suitable works for algae on permanent snowfields or glaciers.

The Greenland Ice Sheet, the second largest continuous body of ice in the world, is known to be inhabited by snow algae. Several studies have reported the visible red snow caused by blooms of *Cd. nivalis* over the ice sheet (Lutz et al., 2014; Uetake et al., 2010; Takeuchi et al., 2014). The ice sheet is reportedly losing mass due to an increase in temperature and decrease in surface albedo during the last two decades (Rignot et al., 2008; Wientjes and Oerlemans, 2010; Box et al., 2012). Decline in snow surface albedo by algal blooms might have increased surface melting rates and decreased mass of the ice sheet in recent years (Yallop et al., 2012; Aoki et al., 2013; Lutz et al., 2016). Observation of a glacier in south east Greenland showed surface albedos for red snow (49%) to be lower than that of clean snow (75%), and that snow algal growth might lead to a positive feedback, increasing the melting rate of the glacier (Lutz et al., 2014). Quantification of snow algal abundance is important for estimating the melting rate of snow over the ice sheet. However, there is little information on the temporal changes in snow algal abundance on a snowpack in Greenland, and a numerical model for the snow algal growth has not been established to date.

In this study, biological and meteorological observations were conducted on the Qaanaaq Glacier located in north west Greenland in order to quantify the temporal change in snow algal abundance and establish a numerical model for algal growth. Temporal changes in algal abundance on the snow surface were quantified at two locations on the glacier from June to August



in 2014 and were fitted to a simple numerical equation. Factors affecting the parameters of the equation are discussed in terms of meteorological data and, physical and chemical snow data from the study sites.

2 Study sites and methods

The investigation was conducted at the Qaanaaq Ice Cap in northwest Greenland (Fig. 1) from June to August in 2014. The Qaanaaq Ice Cap, which lies on a small peninsula of north west Greenland, covers an area of 286 km² and has an elevation of approximately 1,110 m a.s.l. (Takeuchi et al, 2014; Sugiyama et al, 2014). We selected two study sites at different elevations (Sites-A and B) on the Qaanaaq Glacier, which is an outlet glacier of the ice cap and is easily accessible on foot from Qaanaaq village. Site-A is a snowpack located at an elevation of 551 m a.s.l. towards the middle of the glacier and is likely formed by snowdrift. Since the depth of the snowpack was deeper than that of surrounding areas, the snow persisted through much of the melting season. Site-B is located at 944 m a.s.l., and was close to the equilibrium line of the glacier (Tsutaki et al., 2017). Meteorological data used in the study were collected with an automatic weather station (AWS), which was installed at Site-B in 2012 by the Snow Impurity and Glacier Microbe effects on abrupt warming in the Arctic project (SIGMA) (Aoki et al., 2014). Air temperature and solar radiation were collected hourly from April to August 2014 using the AWS. Aoki et al. (2014) provided a more detailed description of the AWS. The temperature sensor and pyranometer of the AWS were placed at heights of 3.0 m and 2.5 m above the snow surface, respectively. Air temperature at Site-A was calculated from the air temperature collected at Site-B with a temperature lapse rate, which was assumed as $-7.80 \times 10^{-3} \text{ K m}^{-1}$ (Sugiyama et al., 2014). Solar radiation at Site-A was measured hourly from day 172 (21 June 2014) to 214 (2 August 2014) with a pyranometer (EKO ML-020) installed at 1.5 m above the snow surface. The measured time of the hourly meteorological data is defined as Local Time (LT = Greenwich Time – 2 h) in summer.

Snow pits were observed once weekly during the study period at both sites to determine vertical profiles of snow type, temperature, density, and liquid-water content. The snow temperature was measured with a thermistor sensor (CT-430WP, Custom Ltd, Tokyo, Japan). The volumetric liquid-water content in snow layers was obtained from snow density and snow permittivity, which were measured using a density sampler and dielectric probe (Denoth, 1994), respectively. Snow surface temperature was obtained from direct measurements and from calculating the observed downward and upward longwave radiant fluxes assuming the emissivity of the snow surface to be 0.98 (Armstrong and Brun, 2008), following the protocol of Niwano et al. (2015).

Surface snow collection and snow pit observation were performed, simultaneously from days 162 to 214 (nine times total) at Site-A and from days 168 to 215 (eight times total) at Site-B. Samples were collected from one to five randomly selected surfaces (depth of 0 cm to 2 cm) using a stainless-steel scoop. The sampling area ranged from 100 to 900 cm² and was recorded for each collection. All snow samples were preserved in Whirl-Pak® bags (Nasco, Fort Atkinson, Wisconsin, USA). Electrical conductivity (EC) and pH for the collected samples were measured using a portable pH-conductivity meter (F-54, HORIBA, Japan) after the samples were melted in Qaanaaq village. Samples used for algal cell analysis were collected separately. These



samples were melted and preserved in 3% formalin in 30 ml clean polyethylene bottles before being transported to Chiba University, Japan, for analysis.

Algal abundance was obtained by cell counting and was represented as cell numbers per unit surface area of snowpacks. Water samples of 20–1000 μl were filtered through a hydrophilized PTFE membrane filter (pore size 0.45 μm , Millipore). The number of algal cells on the filter was counted two to five times for each sample using an optical microscope (BX51, OLYMPUS, Japan) and cell concentration (cells L^{-1}) were obtained from mean cell counts and filtered sample volumes. Cell numbers per unit area (cells m^{-2}) were calculated using the cell concentration and area of sample collection. To obtain a cell volume biomass (biovolume), mean cell volumes were estimated by measuring the size of 5–50 cells for each species using a microscope and mean cell volume was obtained geometrically. Total algal volume per unit area (mL m^{-2}) per taxon was obtained by the multiplying cell count and cell volume.

Abundance of mineral particles in snow was quantified using another set of samples collected from the snow surface. Melted samples were dried (60°C, 24 h) in pre-weighed crucibles then combusted (500°C, 3h) in an electric furnace to remove organic matter. The mass of mineral particles per area (g m^{-2}) was obtained from the combusted sample weight and sampling area since only mineral particles remained after combustion.

15 3 Results

3.1 Meteorological conditions

Meteorological observations on the Qaanaaq Glacier showed that air temperature was below 0°C from April through most of June and increased above 0°C from late June through early August (Fig. 2a). The daily mean air temperature at Site-B ranged from -25.8°C to -11.1°C in April and from -19.7°C to -7.9°C in May. It first exceeded 0°C in daytime on day 154 (3 June 2014) and remained above 0°C from late June to early August. This air temperature record indicates that snow melting occurred continuously from late June to August at the study sites.

Solar radiation gradually increased from April to mid-July, before decreasing (Fig. 2b). At the location of the Qaanaaq Glacier, the sun never set from day 108 (18 April 2014) to day 241 (29 August 2014). Monthly mean solar radiation at Site-B for April, May, June, and July was 165, 276, 296, and 244 W m^{-2} , respectively. The daily mean solar radiation in July ranged from 71 and to 375 W m^{-2} (mean: 218 W m^{-2}) and from 90 to 383 W m^{-2} (mean: 244 W m^{-2}) at Sites-A and B respectively, indicating that the solar radiation did not significantly vary among sites.

3.2 Physical and chemical conditions of surface snow

Snow observations showed that the surface snow was consistently wet from late June to early August at both sites (Figs. 3 and 4). When the observation was started on day 168 (17 June 2014), the surface snow at Site-B was fresh dry snow without surface melt. This snow became granular on day 176, implying that the snow surface began to melt. Surface snow density was 386 kg m^{-3} on day 168 and gradually increased until day 215 (3 August 2014, 489 kg m^{-3}). The mean snow grain size was 0.3 mm on



day 168, 0.9 mm on day 181, and varied between 0.7 and 0.9 mm until day 215. Snow surface level decreased by 121 cm during the study period (47 days). Surface snow temperature was -0.2°C on day 168 and 0°C from days 176 to 215, except day 197 (-0.1°C). Hourly surface snow temperature was calculated from longwave radiation and showed that the duration temperature was above 0°C for 885 h of 1129 h during the study period. The volumetric liquid-water content of surface snow was 6.3% on day 181 and varied between 3.8 and 4.9% until day 215. Changes in snow properties were similar between sites. For example, the surface snow of Site-A was granular and the surface snow temperature was 0°C after day 179. The results indicate that the snowpacks at both sites melted continuously from late June until early August.

The mass of mineral particles in surface snow gradually increased from June to early August at both sites, and it was consistently greater at the lower site (Site-A) than at the higher site (Site-B) (Figs. 3 and 4). The mineral abundance at Site-B was $3.0 \times 10^{-3} \text{ g m}^{-2}$ on day 176 and gradually increased to $7.6 \pm 3.0 \times 10^{-1} \text{ g m}^{-2}$ (mean \pm SD) until day 215. The abundance at Site-A was 1.4 g m^{-2} on day 179 and gradually increased to $6.6 \pm 1.9 \text{ g m}^{-2}$ until day 214. A statistical test demonstrated that the temporal changes in mineral abundance were significant at both sites (one-way ANOVA, Site-B: $F = 4.95$, $P = 0.02 < 0.05$; Site-A: $F = 2.74$, $P = 0.004 < 0.01$). The comparison of the mineral abundance in August between Sites-A and B showed that their difference was statistically significant. (6.6 ± 1.9 vs. $7.6 \pm 3.0 \times 10^{-1} \text{ g m}^{-2}$; Student's t -test, $t = 4.10$, $P = 0.009 < 0.01$).

The EC and pH of surface snow did not show seasonal trends or differences between the sites. The EC ranged from 1.5 to $4.0 \mu\text{S cm}^{-1}$ (mean: $2.7 \mu\text{S cm}^{-1}$) and from 0.4 to $3.2 \mu\text{S cm}^{-1}$ (mean: $2.4 \mu\text{S cm}^{-1}$) at Sites-A and B, respectively. The pH ranged from 5.5 to 6.2 (mean: 5.9) and from 5.3 to 6.1 (mean: 5.8) at Sites-A and B, respectively. There was no significant difference in EC or pH between sites in late June (Student's t -test, EC: $t = 2.47$, $P = 0.13 > 0.05$; pH: $t = 2.32$, $P = 0.15 > 0.05$). The EC and pH in July and August did not significantly vary among sites.

3.3 Snow algae on snow surface

Microscopic observation revealed that the red spherical algal cells were dominant at both study sites. Algal cells (Fig. 5) contained a reddish-orange and/or green pigment and were $21.3 \pm 2.3 \mu\text{m}$ in diameter. The cell volume biomass of this alga accounted for over 95% of the total algal biomass at both study sites. This alga was likely *Chlamydomonas (Cd.) nivalis* since the shape, size, and pigmentation (Fig. 5) corresponded with the taxon observed previously in 2007 and 2012 on this glacier (Uetake et al., 2010; Takeuchi et al., 2014).

The other cell types were present in the samples in trace amount. One was spherical in shape with orange or green pigment, and its cell size was smaller ($9.0 \pm 2.2 \mu\text{m}$) than the previously described algae. Another cell was also spherical but with pale blue-green pigments and was much smaller in size ($4.6 \pm 1.2 \mu\text{m}$). These types of algal cells were likely the undefined alga and *Chroococcaceae cyanobacterium* reported by Uetake et al. (2010), respectively.

3.4 Temporal changes in algal cell concentration of surface snow

Microscopic analysis revealed that the algal cell appeared on the surface snow in late June and gradually increased until late July (Fig. 6). Algal abundance was 7.4 cells m^{-2} at Site-B when the algae first appeared on day 181 and then increased to 5.0



$\times 10^5$ cells m^{-2} until day 215, although abundance decreased occasionally on days 190 and 197 (Fig. 6b). The algal cells at Site-A first appeared on day 179 (3.1×10^3 cells m^{-2}), then their abundance exponentially increased until day 201 (2.2×10^7 cells m^{-2}) (Fig. 6a). Temporal changes in algal abundance were significant at both sites (one-way ANOVA, Site-A: $F = 2.45$, $P = 0.006 < 0.01$; Site-B: $F = 2.91$, $P = 5.9 \times 10^{-5} < 0.01$).

5 The algal abundances on the snow surface at Site-B continued increasing until early August, whereas the abundances at Site-A did not significantly increase between days 201 to 214 (Fig. 6). The mean algal abundance at Site-A was 2.2×10^7 cells m^{-2} on day 201 and 3.5×10^7 cells m^{-2} on day 214. The algal abundance on day 201 was 637 times that of day 195; however, algal abundance on day 214 was only 1.6 times that of day 201. The temporal change in algal abundance at Site-A was not significant between days 201 and 214 (one-way ANOVA, $F = 4.56$, $P = 0.26 > 0.01$).

10

4 Discussions

4.1 Origin of snow algae and their growth condition on the Qaanaaq Glacier

The red snow phenomenon observed on the Qaanaaq Glacier is likely to occur every summer according to previous studies on the glacier (Uetake et al., 2010; Takeuchi et al., 2014). Additionally, the species causing this phenomenon are likely the same
15 as those typically occurring in Arctic snowfields. The dominant algal cell, *Cd. nivalis*, has been widely reported in Arctic snowfields (Spijkerman et al., 2012; Takeuchi, 2013; Hisakawa et al., 2015; Lutz et al., 2016; Tanaka et al., 2016).

The red algal cells appear to have originated from windblown algal spores in the atmosphere, but they are not likely from the remaining snow of previous melting season. Algae growing on the snow surface are usually derived from spores transported by wind or animals from distant places (up to hundreds or kilometers) or from motile cells that migrated from the lower layers
20 of the snowpack (Müller et al., 2001; Remias, 2012). The migration of motile cells in the snowpack requires solar radiation as well as liquid water (Hoham, 1980). However, incident active radiation can only penetrate to a depth of 1 m in wet snowpacks (Curl et al., 1972). When snow algae appeared on the snow surface at the study sites, the previous summer surface was located deeper than 1 m from the present surface (229 cm and 110 cm at Sites-A and B, respectively). The depth appeared to be too great for these cells to migrate to the surface. Furthermore, there was superimposed ice over the last summer surface in the
25 snowpack at Site-B when the algae appeared (Aoki et al., 2014). The superimposed ice layers seem to block algal migration to the surface. Therefore, the algal cells are unlikely to have originated from beneath the snow, but from the atmosphere. Alternatively, algal cells might have been transported from the ground surface surrounding the glacier or from distant sources.

Meteorological records suggest that the initiation of algal growth requires the air temperature to remain above 0°C for a certain period of time after the previous snowfall. The snow algae at both Sites-A and B appeared two days apart from each
30 other. Prior to algal appearances, the hourly air temperature remained above 0°C for 94 h from day 175 at Site-A and for 136 h from day 176 at Site-B; there was no snowfall during this time at either site. The period from the last snowfall appears to be important in initiating snow algal growth, as fresh snow coverage inhibits photosynthesis of the snow algae under the snow.



Additionally, snowmelt is required for the initiation of algal growth (Fukushima, 1963; Onuma et al., 2016). Snow algae on a snowpack in Japan has been reported to appear when air temperatures exceed 0°C for 24 h, which is likely the minimum requirement for initiating snow algal growth (Onuma et al., 2016). The duration was longer in this study than that which was observed in Japan. The longer duration may be due to a difference of algal species or weather conditions on this glacier.
5 Although further studies are necessary to determine the meteorological conditions necessary for the initiation of snow algal growth, these results suggest that continuous melting for a minimum of 94 h is required on the Qaanaaq Glacier.

4.2 Approximation of the algal growth curve with a numerical model

In order to reproduce the observed algal growth with a numerical equation, we applied a logistic model that utilizes a general differential equation of microbial growth to the observed algal growth curve. An increase in microbial cells can simply be expressed by a differential equation known as the Malthusian model, which is defined by an initial cell concentration and algal growth rate (Lavoie et al., 2005). The Malthusian model is based on the assumptions that microbial abundance increases by cell division of all present cells at a constant rate, that there is no addition or removal of cells in the habitat, and that light, nutrients, and habitable space are unlimited. According to this model, the microbial growth curve is calculated as follows (Cui and Lawson, 1982):
15

$$X = X_0 e^{\mu(t-t_0)}, \quad (1)$$

where X and X_0 are population densities of microbes at t and t_0 , respectively, and μ is the growth rate of microbes in t^{-1} . The Malthusian model has been applied to observational microbial abundances in sea ice (Lavoie et al., 2005) and in snowfield (Onuma et al., 2016). However, the algal abundance at Site-A did not significantly increase after late July, despite the air temperature remaining above 0°C and a lack of snowfall, indicating that the Malthusian model could not represent the algal growth curve on the surface snow of the Qaanaaq Glacier. The decreased growth rate observed on the glacier suggests that algal abundance has a limited capacity in this habitat. A logistic model is a microbial growth equation with a carrying capacity, and thus could represent the algal growth curve observed in this study. The temporal change of the logistic model is represented as follows (Cui and Lawson, 1982):
20

$$25 \quad X = \frac{K}{1 + \frac{K-X_0}{X_0} e^{\mu(t_0-t)}}, \quad t = d - d_f, \quad (2)$$

where K is the carrying capacity of algae in the snow surface (depth = 2 cm) and t_0 can be the day of the first appearance of algae on the snow surface. Since snow algae can grow only on the melting snow surface, we assumed that algal growth was interrupted when snow surface temperature was below 0°C. Thus, t represents the number of the days during which the mean temperature was above 0°C. This equation was fitted to the observational algal cell concentrations at Sites-A and B through Poisson regression. The observational data used are from the day of algal appearance (days 179 at Site-A and 181 at Site-B, t_0) through the last day of the study period (days 214 at Site-A and 215 at Site-B, t_{max}). This regression is based on the assumption that there is no inflow or outflow of algal cells on the snow surface. Although the algal abundance on surface snow
30



is possibly affected by algal cells carried by wind and from deeper snow, such effects appeared to be small enough to calculate algal growth because the initial concentration of algae on the surface (3.1×10^3 cells m^{-2} on day 179 at Site-A), which was likely due to wind, was substantially smaller than the final concentration (3.5×10^7 cells m^{-2} on day 214 at Site-A). To fit Poisson regression to the observed algal cell concentrations, carrying capacity was assumed to be 3.5×10^7 cells m^{-2} at both sites based on the observed maximum concentration of algal cells (day 214 at Site-A). Although it is uncertain whether the algal concentration on day 214 at Site-A was the greatest during the summer, the carrying capacity on the glacier was likely around 3.5×10^7 cells m^{-2} since the cell concentrations of all of algal types hardly increased from day 201 to 214 despite air temperatures remaining above 0°C .

Fitting the data to the model showed that the coefficients of determination of the regression (R^2) were 0.64 and 0.96 at Sites-A and B, respectively, suggesting that the algal growth curve was reproduced with the equation (Table. 1, Figs. 7 and 8). The calculated growth curve at Site-A did not reproduce the reduction of algal cell concentration from days 201 to 208. This is likely the reason for the lower R^2 value at Site-A. However, the calculated algal cell concentration (3.4×10^7 cells m^{-2}) was consistent with the observed abundance (3.5×10^7 cells m^{-2}) at Site-A on day 214, which was the day when algal cell concentration on surface snow was the greatest during the observational period; this suggests that the model can accurately reproduce the timing when algal cell concentration reached the carrying capacity.

4.3 Factors affecting parameters of algal growth model

The growth rates (μ) obtained from the regression of the algal growth curve did not significantly differ between the two sites, whereas the initial cell concentration (X_0) at the lower site was 100 times greater than that of the higher site (Table 1).

The difference in initial cell concentration (X_0) between the two sites was likely attributed to the abundance of initial algal spores supplied from the atmosphere. The initial cell concentration observed at Sites-A and B were 6.9×10^2 cells m^{-2} and 6.3 cells m^{-2} , respectively, and that of Site-A was approximately 100 times more than that of Site-B (Table 1). The abundance of mineral particles on the snow surface was also significantly greater at Site-A (1.4 g m^{-2}) than Site-B ($7.0 \times 10^{-3} \text{ g m}^{-2}$). The sources of mineral particles on the Qaanaaq Glacier were mostly from local sediments, such as soil and moraine near the glacier (Nagatsuka et al., 2014). Therefore, the initial algal spores on surface snow are likely supplied with mineral particles by wind from surrounding ground surface. There is little information on the abundance of initial algal spores on snow surface. Estimation of initial algal concentrations from mineral particle abundance could be applied to this model in the other glaciers or snowfields since the abundance of mineral particles is widely available by observation, the surface mass balance model on the Greenland Ice Sheet (Goelles et al., 2015), and atmospheric circulation models (Ginoux et al., 2001).

The growth rates (μ) obtained from both sites were similar, suggesting that growth rates on the glacier are constant. The growth rates were 0.39 d^{-1} and 0.42 d^{-1} at Sites-A and B, respectively (Table 1). Although solar radiation might affect algal photosynthesis and thus their growth rate on the snowpack, the effect is unclear since there was no significant difference in the July solar radiation among the two sites (218 vs. 244 W m^{-2} for Sites-A and B, respectively). The growth rate of isolated



Chloromonas nivalis in the culture was 0.6 d^{-1} at 18°C water (Leya et al., 2009), which was significantly greater than the growth rate of $0.39\text{--}0.42 \text{ d}^{-1}$ in the present study (Table 1). The lower growth rate in our study is likely due to the lower temperature of the algal habitat compared to the culture conditions, as growth rate of fresh water algae is dependent on water temperature (Eppley, 1972). The growth rate of snow algae may also vary among algal species although further study is
5 necessary.

The carrying capacity of snow algae may be determined by nutrient availability in the snowpack. The carrying capacity was estimated to be $3.5 \times 10^7 \text{ cells m}^{-2}$, based on the observed growth curve in this study (Table 1). Although there are no observational data on the carrying capacity of snow algae, it could be represented by the cell concentration of snow algal bloom reported late in the melting season in previous studies. Cell concentrations of snow algal blooms reported previously in various
10 geographical locations ranged from 5.1×10^7 to $7.5 \times 10^9 \text{ cells m}^{-2}$ (Table 2), suggesting that carrying capacity varies among sites and might be determined by environmental conditions. There are two possible factors affecting carrying capacity: (1) the reduction in physical space available for microbial growth (i.e. the volume of liquid melt water, McKindsey et al., 2006) and (2) the exhaustion of resources for the algae on the snow surface (Cui and Lawson, 1982). The maximum algal cell volume on surface snow (depth = 2 cm) at Site-A (day 214) was substantially smaller compared to the total volume of liquid-water in the
15 surface snow obtained from the water content (0.19 mL m^{-2} vs. 500 mL m^{-2}); this indicates that the physical space for algal growth in the habitat is not a factor affecting carrying capacity in this study. Nutrients such as nitrogen and phosphorus are essential elements for algal growth and are usually supplied from the atmosphere to the snow surface as aerosols. Phosphorus supplied that is carried by wind to glaciers in the form of phosphate minerals easily becomes a limiting factor for algal growth compared to nitrogen, as the concentration of phosphorus was less than that of nitrogen in glaciers (Stibal et al., 2008).
20 Addition of nutrients from outside likely increases snow algal abundance in the snowpacks reported by Ganey et al. (2017). Therefore, the supply of nutrients in the form of mineral dust and/or nitrogen aerosol to the glacier likely determines the carrying capacity in the snowpack, although further study is necessary to substantiate this claim.

5 Conclusions

25 The temporal changes in snow algal abundance on snowpacks of the Qaanaaq Glacier in northwest Greenland were studied. Spherical algal cells filled with red pigment, which are likely *Cd. nivalis*, were dominant on the snowpack. The algal cells first appeared on the snow surface in late June when snow from the previous season had melted and the air temperature remained above 0°C exceeded for approximately 94 h. Algal abundance increased exponentially for a month, and then the growth rate decreased mid-July, even though the air temperatures remained above 0°C and no snowfall occurred. A logistic model was
30 applied to the observed algal growth curves to reproduce abundance numerically using three parameters; the initial cell concentration (X_0), growth rate (μ), and carrying capacity (K). The growth curves were reproduced accurately with coefficients of determination (R^2) of 0.64 and 0.96 at the lower and higher sites, respectively. Our observational results suggest that the



model parameters can be determined using the environmental conditions (physical and chemical snow properties and meteorological conditions) of the glacier; thus, this logistic model could be applied to the snow algae on various glaciers and snowfields. Although more research is necessary to validate the model, our results demonstrate that this simple numerical model could simulate the temporal variation in algal abundance on snow surface. This model is useful for quantifying algal growth on snowpacks worldwide, physical snow models or global climate models, and evaluating the effects of algae on the surface albedos and melting rates of snowpacks.

6 Acknowledgements

We would thank to the field campaign members of the SIGMA (Snow Impurity and Glacial Microbe effects on abrupt warming in the Arctic) project and GRENE (the Green Network of Excellence) Arctic Climate Change Research project in Greenland in 2014. This study was supported in part by Grant-in-Aids (23221004, 26247078, 26241020, 16H01772).

References

Aoki, T., Kuchiki, K., Niwano, M., Matoba, S., Uetake, J., Masuda K., and Ishimoto, H.: Numerical Simulation of Spectral Albedos of Glacier Surfaces Covered with Glacial Microbes in Northwestern Greenland, RADIATION PROCESSES IN THE ATMOSPHERE AND OCEAN (IRS2012), Robert Cahalan and Jürgen Fischer (Eds), ALP Conf. Proc., 1531, 176, doi:10.1063/1.4804735, 2013.

Aoki, T., Matoba, S., Uetake, J., Takeuchi, N., and Motoyama, H.: Field activities of the “Snow Impurity and Glacial Microbe effects on abrupt warming in the Arctic” (SIGMA) project in Greenland in 2011–2013, Bull. Glaciol. Res., 32, 3–20, doi:10.5331/bgr.32.3, 2014.

Box, J. E., Fettweis, X., Stroeve, J. C., Tedesco, M., Hall, D. K., and Steffen, K.: Greenland ice sheet albedo feedback: thermodynamics and atmospheric drivers, The Cryosphere, 6, 821–839, doi:10.5194/tc-6-821-2012, 2012.

Chen, S., Chen, X., Peng, Y., and Peng, K.: A mathematical model of the effect of nitrogen and phosphorus on the growth of blue-green algae population, Appl. Math. Model., 33, 1097–1106, doi:10.1016/j.apm.2008.01.001, 2009.

Cook, J. M., Hodson, A. J., Taggart, A. J., Mernild, S. H., and Tranter, M.: A predictive model for the spectral “bioalbedo” of snow, J. Geophys. Res. Earth Surf., 122, doi:10.1002/2016JF003932, 2017.



- Cook, J., Hodson, A., Gardner, A., Flanner, M., Tedstone, A., Williamson, C., Irvine-Fynn, T., Nilsson, J., Bryant, R., and Tranter, M.: Quantifying bioalbedo: A new physically-based model and critique of empirical methods for characterizing biological influence on ice and snow albedo, *The Cryosphere.*, doi:10.5194/tc-2017-73, 2017.
- 5
- Cui, Q., and Lawson, G. J.: Study on models of single populations: an expansion of the logistic and exponential equations, *J. Theor. Biol.*, 98, 645–659, doi:10.1016/0022-5193(82)90143-6, 1982.
- Curl, H. Jr., Hardy, J.T., and Ellermeier, R.: Spectral absorption of solar radiation in alpine snow fields, *Ecology*, 53, 1189–
10 1194, doi:10.2307/1935433, 1972.
- Denoth, A.: An electronic device for long-term snow wetness recording, *Ann. Glaciol.*, 19, 104-106, 1994.
- Eppley, R. W.: Temperature and phytoplankton growth in the sea, *Fish. Bull.*, 70, 1063–1085, 1972.
- 15
- Fukushima, H.: Studies on cryophytes in Japan, *J. Yokohama Munic. Univ. Ser. C, Nat. Sci.*, 43, 1–146, 1963.
- Ganey, G. Q., Loso, M. G., Burgess, A. B., and Dial, R. J.: The role of microbes in snowmelt and radiative forcing on an Alaskan icefield, *Nature Geoscience*, doi:10.1038/NGEO3027, 2017.
- 20
- Ginoux, P., Chin, M., Tegen, I., Prospero, J., Holben, B., Dubovik, O., and Lin, S.-J.: Sources and global distributions of dust aerosols simulated with the GOCART model, *J. Geophys. Res.*, 106, 20,255–20,273, doi:10.1029/2000JD000053, 2001.
- Goelles, T., Bøggild, C. E., and Greve, R.: Ice sheet mass loss caused by dust and black carbon accumulation, *The Cryosphere*,
25 9, 1845–1856, doi:10.5194/tc-9-1845-2015, 2015.
- Hisakawa, N., Quistad, S. D., Hestler, E. R., Martynova, D., Maughan, H., Sala, E., Gavrilo, M. V., and Rowher, F.: Metagenomic and satellite analyses of red snow in the Russian Arctic, *Peer J*, 3, e1491, doi:10.7717/peerj.1491, 2015.
- 30
- Hoham, R. W.: Unicellular chlorophytes-snow algae, *Phytoflagellates* (Cox ER, ed), 61–84, Elsevier, New York, 1980.
- Hoham, R. W., Roemer, S. C., and Mullet, J. E.: The life history and ecology of the snow alga *Chloromonas brevispina* comb. nov. (Chlorophyta, Volvocales), *Phycologia*, 18, 55–70, doi:10.2216/i0031-8884-18-1-55.1, 1979.



- Hoham, R. W., Yatsko, C. P., Germain, L., and Jones, H. G.: Recent discoveries of snow algae in upstate New York and Québec Province and preliminary reports on related snow chemistry, Proc. 46th Ann. Eastern Snow Conf., 196–200, 1989.
- Hoham, R. W., and Duval, B.: Microbial ecology of snow and freshwater ice, in: Jones, H. G., Pomeloy, J. W., Walker, D. A. and Hoham, R. W. (Eds.), Snow Ecology, Cambridge University Press, 168–228, 2001.
- Lavoie, D., Denman, K., and Michel, C.: Modeling ice algal growth and decline in a seasonally ice-covered region of the Arctic (Resolute Passage, Canadian Archipelago), J. Geophys. Res., 110, C11009, doi:10.1029/2005JC002922, 2005.
- 10 Leya, T., Rahn, A., Lütz, C., and Remias, D., Response of arctic snow and permafrost algae to high light and nitrogen stress by changes in pigment composition and applied aspects for biotechnology, FEMS Microbiol. Ecol., 67, 432–443, doi: 10.1111/j.1574-6941.2008.00641.x, 2009.
- Ling, H. U., and Seppelt, R. D.: Snow algae of the Windmill Island, continental Antarctica. *Mesotaenium berggrenii* (Zygnematales, Chlorophyta), the alga of grey snow, Antarct. Sci., 2, 143–148, doi:10.1017/S0954102090000189, 1990.
- 15 Ling, H. U. and Seppelt, R. D.: Snow algae of the Windmill Island, continental Antarctica. 2. *Chloromonas rubroleosa* sp. nov. (Volvocales, Chlorophyta), an alga of red snow, Eur. J. Phycol., 28, 77–84, doi: 10.1080/09670269300650131, 1993.
- 20 Lutz, S., Anesio, A. M., Jorge Villar, S. E., and Benning, L. G.: Variations of algal communities cause darkening of a Greenland glacier, FEMS Microbiol. Ecol., 89, 402–414, doi: 10.1111/1574-6941.12351, 2014.
- Lutz, S., Anesio, A. M., Raiswell, R., Edwards, A., Newton, R. J., Gill, F., and Benning, L. G.: The biogeography of red snow microbiomes and their role in melting arctic glaciers, Nature Communications, doi:10.1038/ncomms11968, 2016.
- 25 McKindsey, C. W., Thetmeyer, H., Landry, T., and Silvert, W.: Review of recent carrying capacity models for bivalve culture and recommendations for research and management, Aquaculture. 261, 451–462, doi:10.1016/j.aquaculture.2006.06.044, 2006.
- 30 Müller, T., Leya, T. and Fuhr, G.: Persistent Snow Algal Fields in Spitsbergen: Field Observations and a Hypothesis about the Annual Cell Circulation, Arct. Antarct. Alp. Res., 33, 42–51, doi:10.2307/1552276, 2001.



- Niwano, M., Aoki, T., Matoba, S., Yamaguchi, S., Tanikawa, T., Kuchiki, K., and Motoyama, H.: Numerical simulation of extreme snowmelt observed at the SIGMA-A site, northwest Greenland, during summer 2012, *The Cryosphere*, 9, 971–988, doi:10.5194/tc-9-971-2015, 2015.
- 5 Onuma, Y., Takeuchi, N., and Takeuchi, Y.: Temporal changes in snow algal abundance on surface snow in Tohkamachi, Japan, *Bull. Glaciol. Res.*, 34, 21–31, doi:10.5331/bgr.16A02, 2016.
- Pogson, L., Tremblay, B., Lavoie, D., Michel, C., and Vancoppenolle, M.: Development and validation of a one-dimensional snow–ice algae model against observations in resolute passage, Canadian Arctic Archipelago, *J. Geophys. Res.*, 116, C04010, doi: 10.1029/2010JC006119, 2011.
- 10 Pollock, R.: What colors the mountain snow?, *Sierra Club Bull.*, 55, 18–20, 1970.
- Remias, D., Lütz-Meindl, U., Lütz, C.: Photosynthesis, pigments and ultrastructure of the alpine snow alga *Chlamydomonas nivalis*, *Eur. J. Phycol.*, 40 (3), 259–268, doi:10.1080/09670260500202148, 2005.
- 15 Remias, D.: Cell structure and physiology of alpine snow and ice algae, In Lütz, C. (Editor) *Plants in alpine regions, Cell physiology of adaption and survival strategies*. Springer Wien, 202, 175–186, doi:10.1007/978-3-7091-0136-0_13, 2012.
- 20 Rignot, E., Box, J. E., Burgess, E. and Hanna, E.: Mass balance of the Greenland ice sheet from 1958 to 2007, *Geophys. Res. Lett.*, 35, L20502, doi:10.1029/2008gl035417, 2008.
- Segawa, T., Miyamoto, K., Ushida, K., Agata, K., Okada, N., and Koshima, S.: Seasonal Change in Bacterial Flora and Biomass in Mountain Snow from the Tateyama Mountains, Japan, Analyzed by 16S rRNA Gene Sequencing and Real-Time PCR, *App. Environ. Microbiol.*, 71 (1), 123–130. doi:10.1128/AEM.71.1.123–130, 2005.
- 25 Spijkerman, E., Wacker, A., Weithoff, G. and Leya, T.: Elemental and fatty acid composition of snow algae in Arctic habitats, *Front. Microbiol.*, 3, 380, doi:10.3389/fmicb.2012.00380, 2012.
- 30 Stibal, M., Tranter, M., Telling, J. and Benning, L. G.: Speciation, phase association and potential bioavailability of phosphorus on a Svalbard glacier, *Biogeochemistry*, 90, 1–13, doi:10.1007/s10533-008-9226-3, 2008.
- Sugiyama, S., Sakakibara, D., Matsuno S., Yamaguchi, S., Matoba, S., and Aoki T.: Initial field observations on Qaanaaq ice cap, northwestern Greenland, *Ann. Glaciol.*, 55, 25–33, doi:10.3189/2014AoG66A102, 2014.



Sutton, F.A.: The physiology and life histories of selected cryophytes of the Pacific NorthWest, Ph.D. Thesis, Oregon State University, Corvallis, 98, 1972.

- 5 Takeuchi, N.: Seasonal and altitudinal variations in snow algal communities on an Alaskan glacier (Gulkana glacier in the Alaska range), *Environ. Res. Lett.*, 8, 035002, doi:10.1088/1748-9326/8/3/035002, 2013.

Takeuchi, N., Dial, R., Kohshima, S., Segawa, T. and Uetake, J.: Spatial distribution and abundance of red snow algae on the Harding Icefield, Alaska derived from a satellite image, *Geophys. Res. Lett.*, 33, L21502, doi:10.1029/2006GL027819, 2006.

10

Takeuchi, N., Nagatsuka, N., Uetake, J., and Shimada, R.: Spatial variations in impurities (cryoconite) on glaciers in northwest Greenland, *Bull. Glaciol. Res.*, 32, 85–94, doi:10.5331/bgr.32.85., 2014.

- 15 Tanaka, S., Takeuchi, N., Miyairi, M., Fujisawa, Y., Kadota, T., Shirakawa, T., Kusaka, R., Takahashi, S., Enomoto, H., Ohata, T., Yabuki, H., Konya, K., Fedorov, A., and Konstantinov, P.: Snow algal communities on glaciers in the Suntar-Khayata Mountain Range in eastern Siberia, Russia, *Polar Sci.*, 10, 3, 227-238, doi:10.1016/j.polar.2016.03.004, 2016.

Thomas, W.H.: Tioga Pass revisited: Interrelationships between snow algae and bacteria, *Proceedings, 62nd Ann. W. Snow Conf.*, Santa Fe, NM, 56-62, 1994.

20

Thomas, W. H., and Duval, B.: Sierra Nevada, California, USA, snow algae: snow albedo changes, algal-bacterial interrelationships, and ultraviolet radiation effects. *Arct. Alp. Res.*, 27, 389–99, doi:10.2307/1552032, 1995.

- 25 Tsutaki S., Sugiyama, S. Sakakibara, D., Aoki, T., and Niwano, M.: Surface mass balance, ice velocity and near-surface ice temperature on Qaanaaq Ice Cap, northwestern Greenland, from 2012 to 2016, *Ann. Glaciol.*, 1-12, doi:10.1017/aog.2017.7, 2017.

Uetake, J., Naganuma, T., Hebsgaard, M. B., and Kanda, H., Communities of algae and cyanobacteria on glaciers in west Greenland, *Polar Sci.*, 4(1), 71-80, doi:10.1016/j.polar.2010.03.002, 2010.

30

Wientjes, I. G. M., and Oerlemans, J., An explanation for the dark region in the western melt zone of the Greenland ice sheet, *The Cryosphere*, 4, 261–268. doi:10.5194/tc-4-261-2010, 2010.



Yallop, M.L., Anesio, A.M., Perkins, R.G., Cook, J., Telling, J., Fagan, D., MacFarlane, J., Stibal, M., Barker, G., and Bellas, C.: Photophysiology and albedo-changing potential of the ice algal community on the surface of the Greenland ice sheet, *ISME J.*, 6, 2302–2313, doi:10.1038/ismej.2012.107, 2012.



Table 1: List of the parameters of a logistic model of snow algal growth obtained from the data of each study site.

Site	Initial cell Concentration X_0 (cells m ⁻²)	Growth rate μ (d ⁻¹)	Carrying capacity K (cells m ⁻²)
Site-A	6.9×10^2	0.42	3.5×10^7
Site-B	6.3	0.39	3.5×10^7



Table 2: List of maximum algal cell concentrations of red algal bloom reported from various snow fields over the world. Maximum algal cell concentrations per area (cells m⁻²) were obtained by calculation from reported maximum algal cell concentrations per volume (cells mL⁻¹) assuming the snow density of granular snow to be 500 kg m⁻³ and the depth of collected samples to be 0.02 m.

Study sites	Algal species	Maximum algal cell concentration (cells m ⁻²)	References
Oregon, USA	<i>Chlamydomonas nivalis</i>	2.3×10^9	Sutton, 1972
Washington, USA	<i>Chloromonas brevispina</i>	5.0×10^9	Hoham et al., 1979
Antarctica	<i>Mesotaenium berggrenii</i>	1.0×10^9	Ling and Seppelt, 1990
Antarctica	<i>Chloromonas rubroleosa</i>	2.0×10^9	Ling and Seppelt, 1993
California, USA	<i>Trochiscia americana</i>	6.3×10^8	Thomas, 1994
Svalbard	<i>Chloromonas alpine</i>	7.5×10^9	Spijkerman et al., 2012
Alaska, USA	<i>Chlyamidomonas nivalis</i>	5.1×10^7	Takeuchi, 2013
SE-Greenland	<i>Chlyamidomonas nivalis</i>	5.0×10^8	Lutz et al., 2014

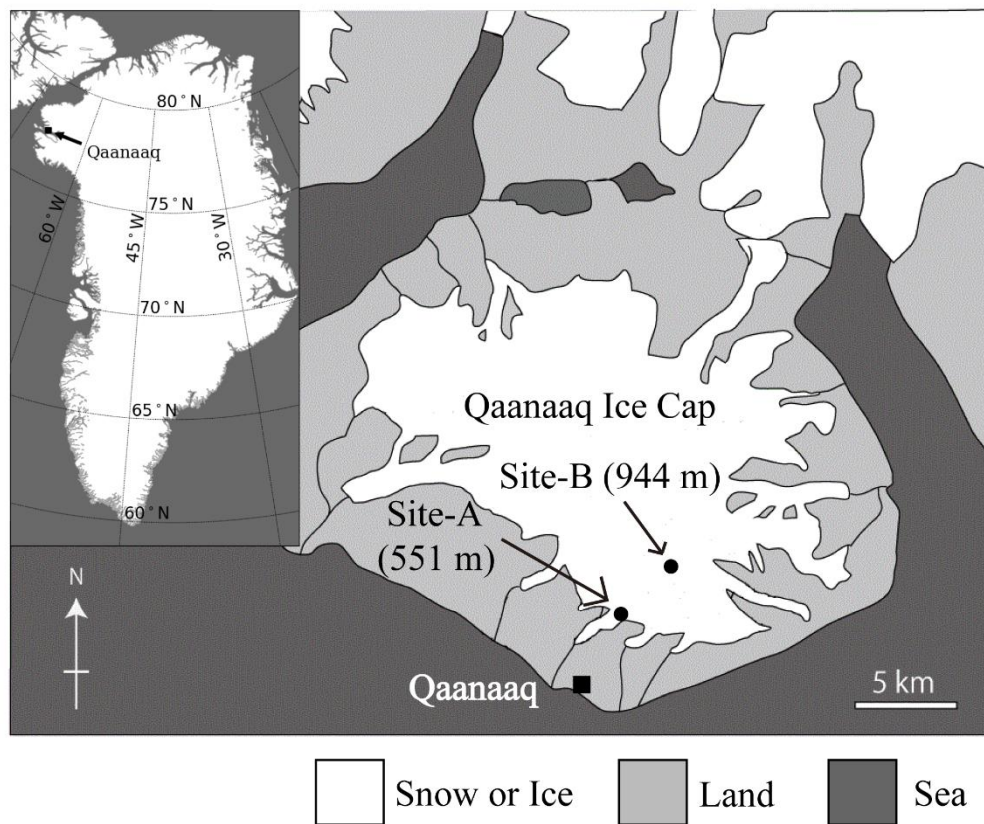


Figure 1: A map of the Qaanaaq Ice Cap in northwest Greenland, showing the location of sampling sites on the glacier.

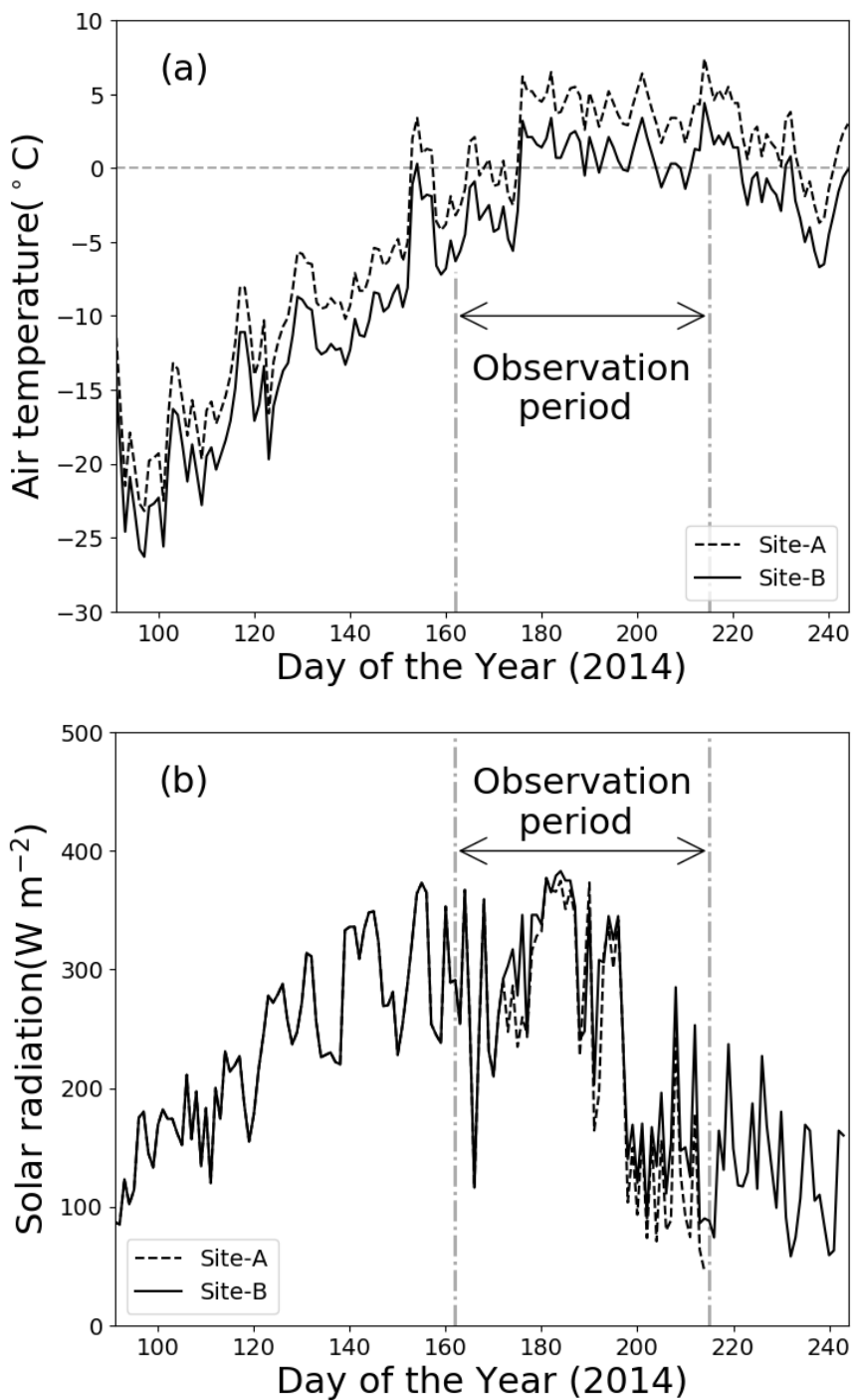


Figure 2: Meteorological conditions at Sites-A and B from 1 April to 1 September 2014. (a) Daily mean air temperature, (b) solar radiation.

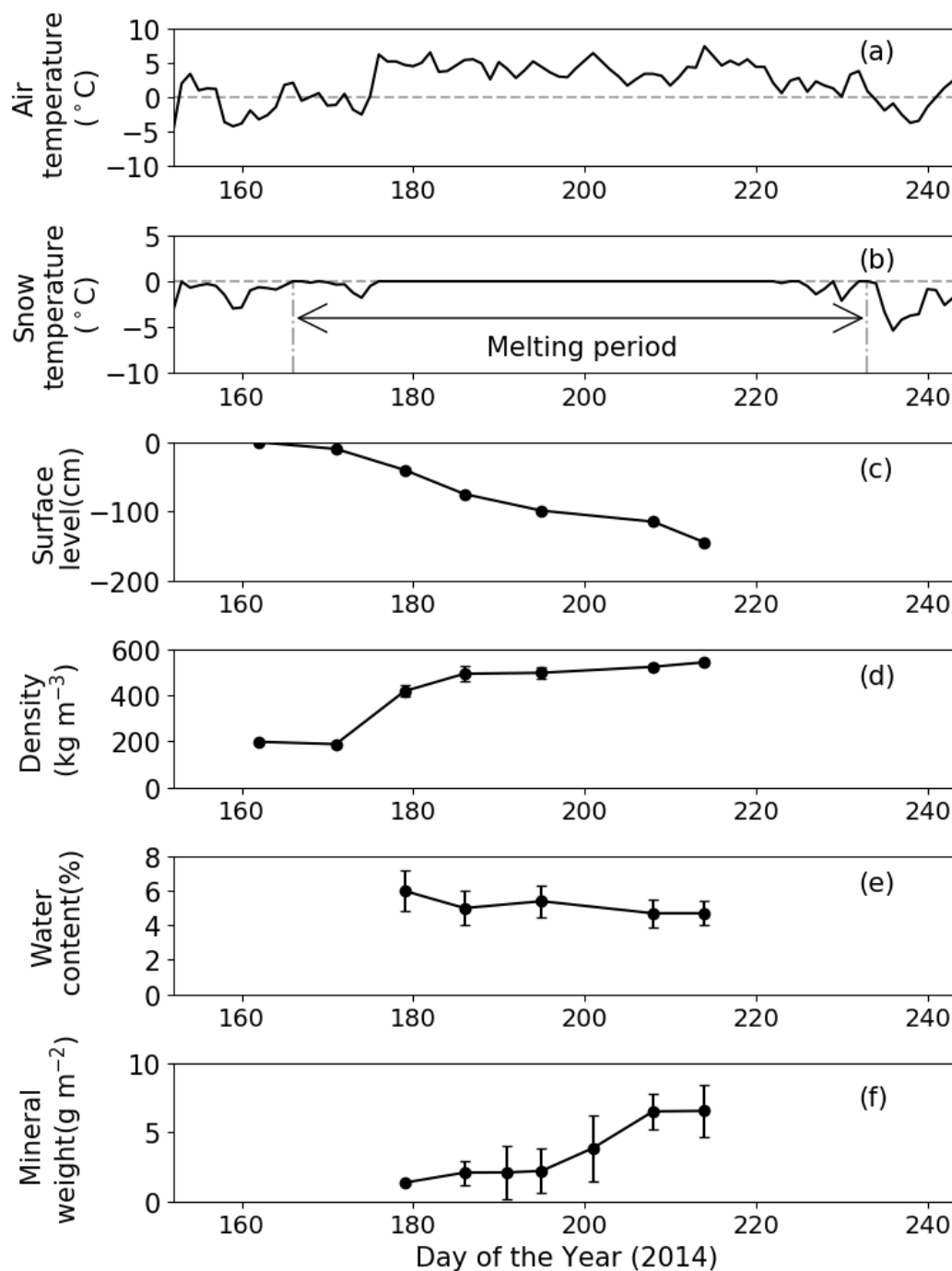


Figure 3: Meteorological and physical conditions of surface snow at Site-A from 1 June to 1 September 2014. (a) Mean daily air temperature, (b) mean daily snow surface temperature calculated from observed downward and upward longwave radiant fluxes, (c) relative snow surface level at the site (0 cm on day 162), (d) snow density, (e) volumetric liquid-water content of snow, and (f) abundance of mineral particles. Melting period in (b) is defined as a period from first day until last day when mean daily snow surface temperature was 0°C from 1 June to 1 September 2014. Standard deviation shown by error bars.

5

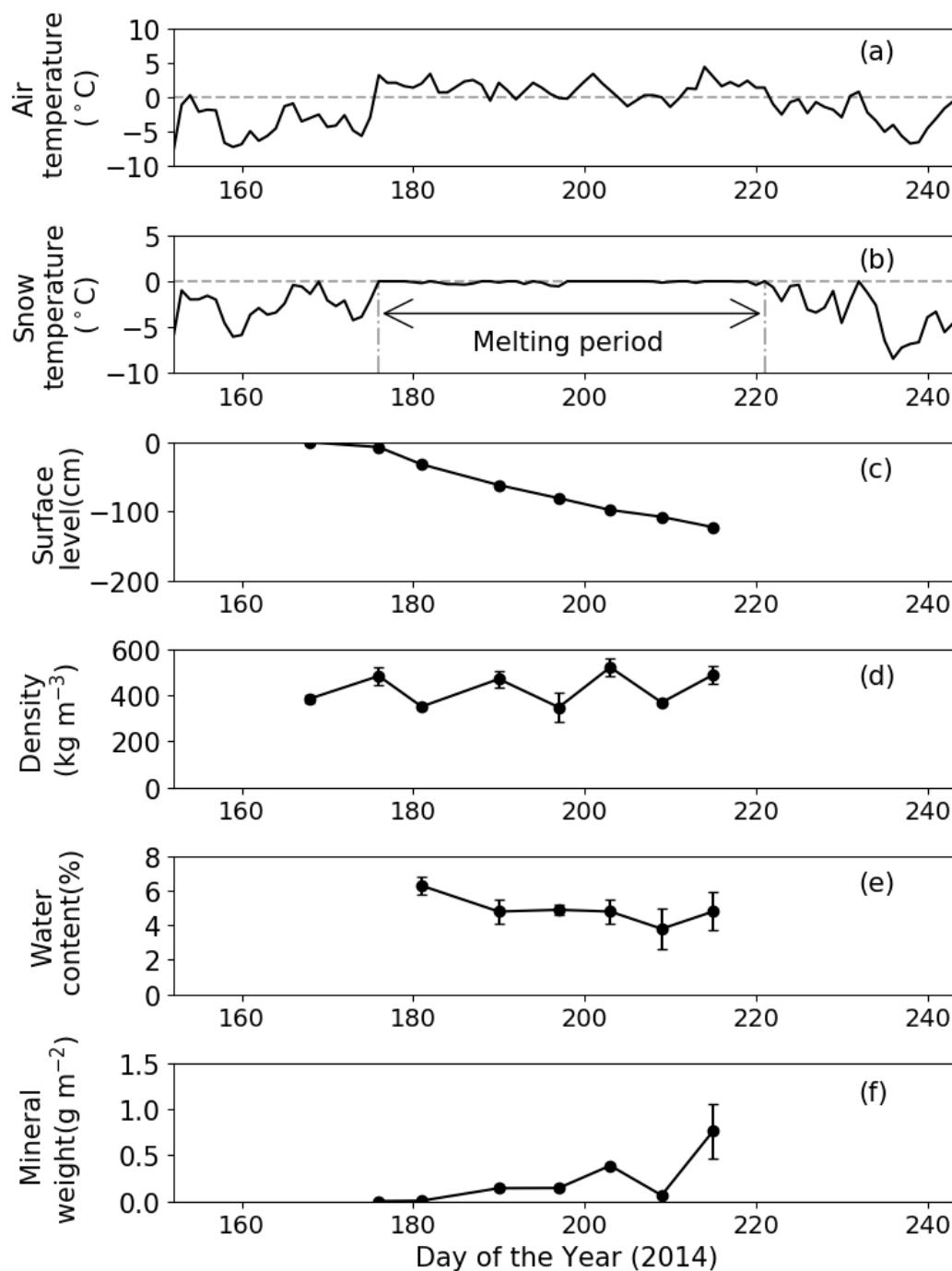


Figure 4: Meteorological and physical conditions on surface snow at Site-B from 1 June to 1 September 2014. (a) Mean daily air temperature, (b) mean daily snow surface temperature calculated from observed downward and upward longwave radiant fluxes, (c) relative snow surface level at the site (0 cm on day 168), (d) snow density, (e) volumetric liquid-water content of snow, (f) abundance of mineral particles. Melting period in (b) is defined as a period from first day until last day when the daily mean snow surface temperature was 0°C from 1 June to 1 September 2014. Standard deviation shown by error bars.

5

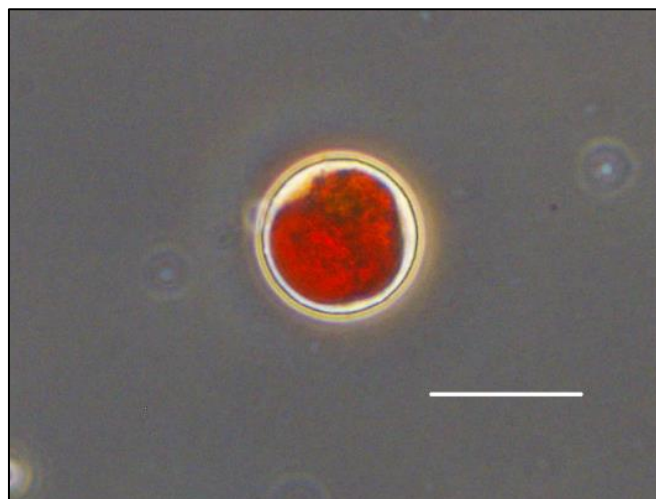


Figure 5: Photograph of snow algal cell observed on the snow surface at Site-A. An oval red cell with secondary carotenoids, most likely mature spores of *Cd. nivalis*, which is the dominant species at both sites. Scale bar = 20 μm .

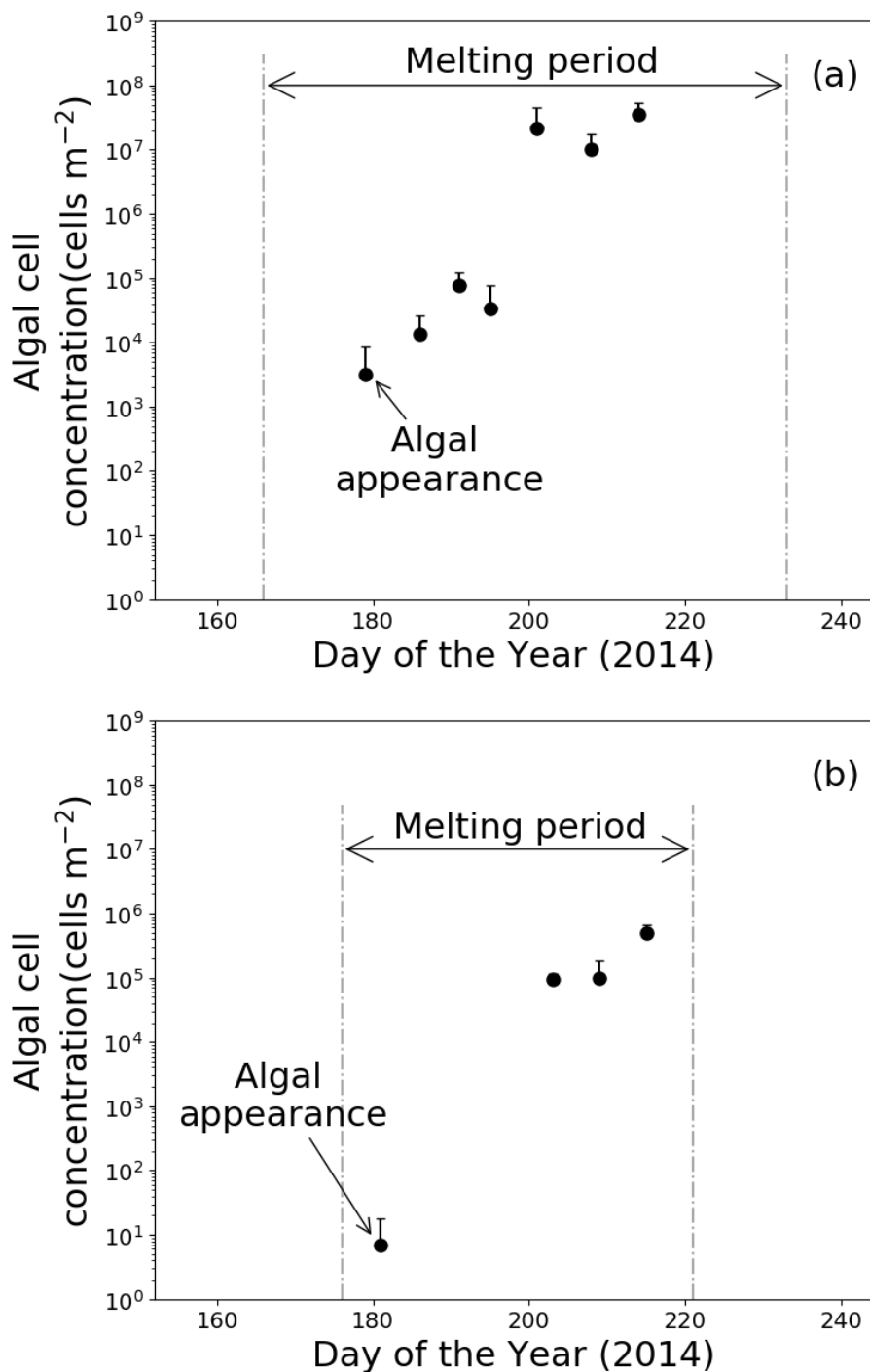


Figure 6: Temporal changes in algal abundance on snow surface at (a) Site-A and (b) Site-B. Melting period in (a) and (b) indicated in Figs. 3 (b) and 4 (b), respectively. Standard deviation shown by error bars.

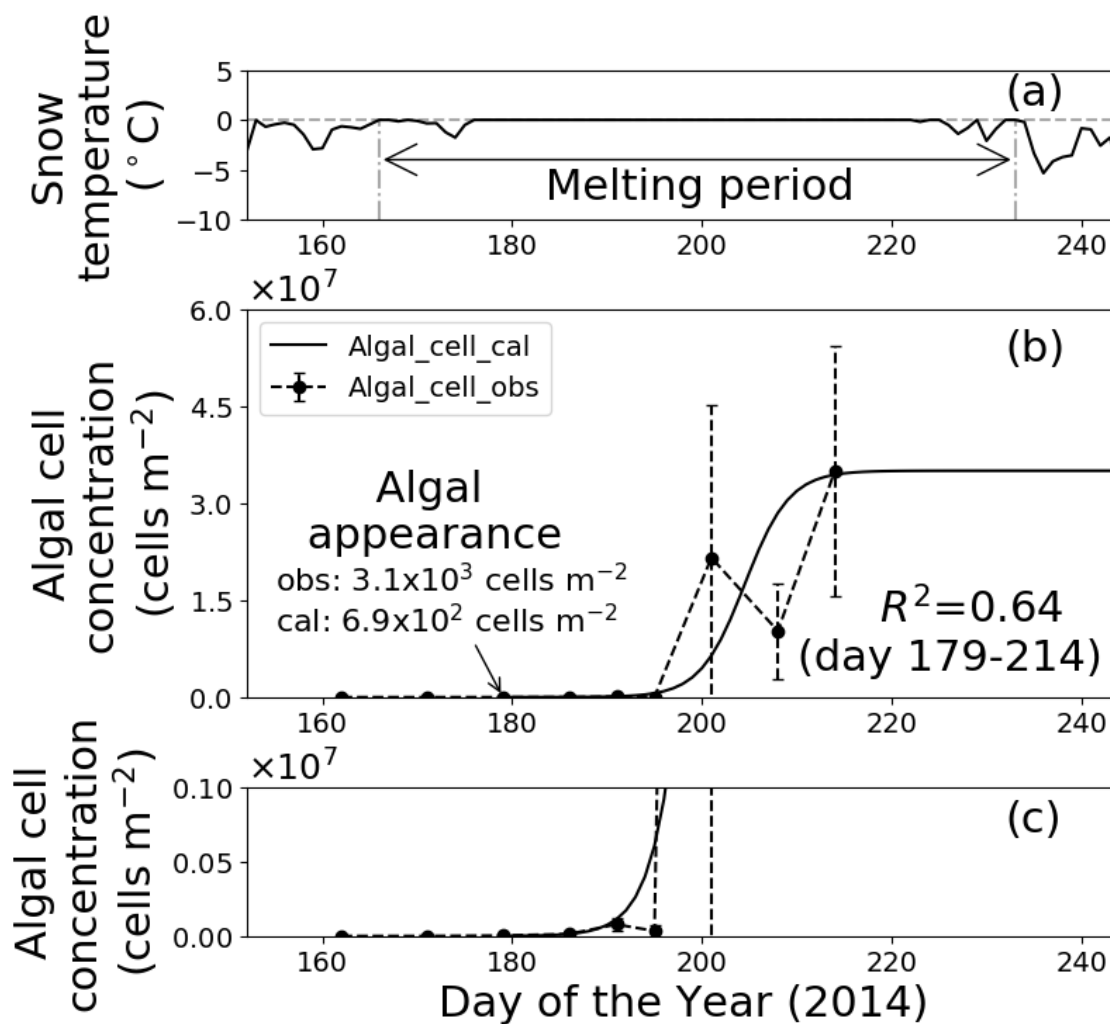


Figure 7: Temporal changes in snow temperature and algal abundance on the surface at Site-A. (a) Mean daily snow surface temperature, (b) observed and calculated algal abundance, and (c) enlargement of the observed and calculated algal abundance between 0 and 1.0×10^6 cells m⁻². Surface snow temperature was calculated from observed downward and upward longwave radiant fluxes. Solid marks indicate observed algal abundance. Solid lines indicate algal abundance calculated from regression by logistic model. Standard deviation shown by error bars.

5

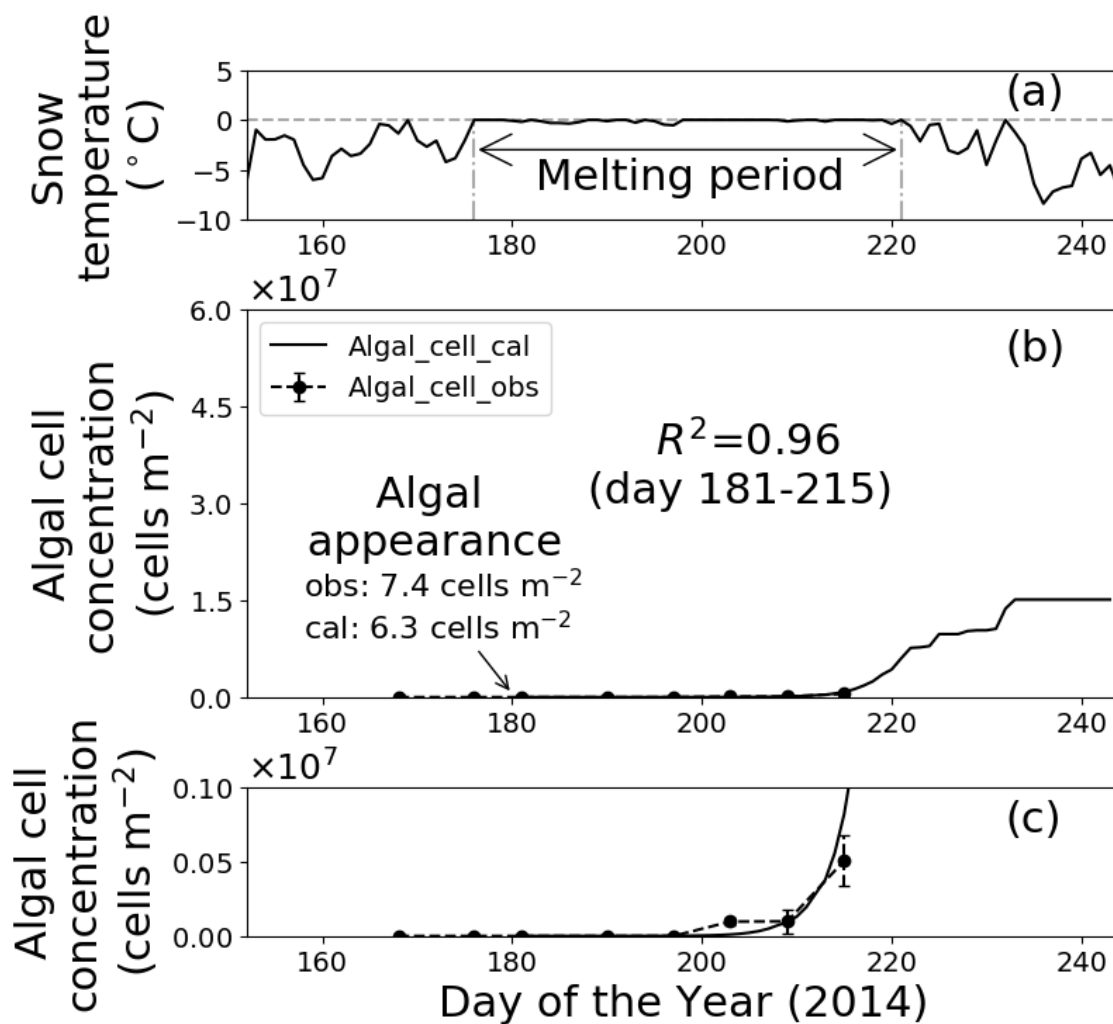


Figure 8: Temporal changes in snow temperature and algal abundance on surface snow at Site-B. (a) Mean daily snow surface temperature, (b) observed and calculated algal abundance, and (c) enlargement of the observed and calculated algal abundance between 0 and 1.0×10^6 cells m⁻². Surface snow temperature was calculated from observed downward and upward longwave radiant fluxes. Solid marks indicate observed algal abundance. Solid lines indicate algal abundance calculated from regression by logistic model. Standard deviation shown by error bars.

5